Dynamics and Mission Design for Space Debris Mitigation in the Geostationary Orbits

By William SILVA,[1)] Maisa TERRA,[1)] Claudia CELESTINO[2)] and Cristiano MELO[3)]

[1)] *Technological Institute of Aeronautics, ITA, São José dos Campos, Brazil*
[2)] *Federal University of ABC, UFABC, Santo André, Brazil*
[3)] *Federal University of Minas Gerais, UFMG, Belo Horizonte, Brazil*

(Received June 21st, 2017)

This work investigates an alternative strategy to divert future communications satellite generations at the end of its operational life exploiting collisional orbits with the Moon. Seeking mitigation strategies of space debris, we explore impulsive transfers between geostationary orbits and lunar gravitational capture orbits in a full 4-body dynamical model with the Sun, Earth, Moon and spacecraft. Criteria to search for natural transfer orbits between the geostationary orbit and the vicinity of the Moon are defined considering escape properties of trajectories of the Circular Restricted Three Body Problem (CR3BP) as a guide. Namely, we select initial conditions of the 4-body model with energies that favors Earth-Moon transfers that remain around the Moon for a long time and eventually collides with the surface of the Moon. As a case of study, we selected the (current) Brazilian geostationary satellite Star One C4. After a large scale analysis of initial conditions and their transport behavior, we select potential transfers that reaches a near vicinity of the GEO orbit with an sufficiently small inclination with respect to the terrestrial equator. Time evolution of candidate solutions are analyzed, as well as Δv budget and propellant mass are computed for space debris mitigation missions. Our removal proposal requires that additional mass of propellant as well as onboard propulsion systems to perform final maneuvers have to be foreseen in the design of future generations of communication satellites.

Key Words: Space Debris, Debris Mitigation, Astrodynamics, Geostationary Orbit

Nomenclature

h	:	Angular Momentum
n	:	Mean motion
m	:	Mass
r	:	Position
$\boldsymbol{r}_j$	:	Vector position of the body j
v	:	Velocity
C_j	:	Jacobi constant
G	:	Universal gravitational constant
$L_i, (i = 1, ..., 5)$:		Lagrange points
N	:	Number of body
P	:	Particle
P_1	:	Primary 1
P_2	:	Primary 2
$\bar{\mu}$	:	Dimensionless mass
$\{0, \eta, \xi, \zeta\}$	:	Inertial reference system (IRS)
$\left\{\dot{\eta}, \dot{\xi}, \dot{\zeta}\right\}$	:	Velocity in the IRS
$\left\{\ddot{\eta}, \ddot{\xi}, \ddot{\zeta}\right\}$	:	Acceleration in the IRS
$\{0, x, y, z\}$	:	Synodic reference system (SRS)
$\{\dot{x}, \dot{y}, \dot{z}\}$	:	Velocity in the SRS
$\{\ddot{x}, \ddot{y}, \ddot{z}\}$	:	Acceleration in the SRS
$\{0, X, Y, Z\}$	:	Heliocentric reference system (HRS)
$\left\{\dot{X}, \dot{Y}, \dot{Z}\right\}$	:	Velocity in the HRS
$\left\{\ddot{X}, \ddot{Y}, \ddot{Z}\right\}$	:	Acceleration in the HRS
Subscripts		
1	:	Sun
2	:	Earth
3	:	Moon
4	:	Spacecraft

1. Introduction

Nowadays space mission design should include the implementation of debris mitigation solutions to preserve the space environment and the sustainability of the project. NASA reports approximately 7,400 metric tons for more than 17,000 objects cataloged in Earth orbit.[1)] Specifically, a guideline proposed by NASA determines some procedures that a satellite must perform at the end of his mission to limit the risk of explosions and collisions after its life span. These practices involve the depletion of the sources of energy and fuel, the prediction of probabilities of collisions with other debris, and the removal of the spacecraft from Low Earth Orbits (LEO), Medium Earth Orbits (MEO) or Geostationary Orbits (GEO).

Debris removal can occur with these possible options: A reentry maneuver in the Earth's atmosphere; a transfer to a graveyard orbit, located between 100 and 300 km above the geostationary orbit;[2)] lunar impact or injection into a heliocentric graveyard orbit.[3)] These rules and policies have had an impact reducing the generation of new debris. But graveyard orbits should be exploited only as short term solutions because the number of objects in these orbits cannot grow indefinitely, in order to avoid the increase of the probability of collisions between objects and the production of clouds of new fragments, some of that could collide with other satellites, resulting in an exponential increase of the production of fragments.[4)] About 400 communication satellites are currently operating in geostationary orbit, while approximately 300 others are out of service and another considerable part in graveyards orbits. However, recent studies show that these graveyards orbits will certainly lead to atmospheric reentry of such debris, so they should be

implemented in a controlled manner to avoid disasters if they fall in large urban centres.[3,5] So, alternative strategies for space debris mitigation are required.

This work aims to seek alternative methods to divert future communication satellites at the end of their operational life through collisional orbits with the Moon. Our main goal is to investigate possible alternative mitigation strategies of space debris in geostationary orbits around the Earth exploiting escape properties of trajectories of the Circular Restricted Three Body Problem (CR3BP)[6–8] and collisional orbits with the Moon. In a preliminary analysis, impulsive transfers between the geostationary orbit and gravitational capture orbit of the Moon guided by the invariant dynamical structures associated to the Lagrangian point L_1 can be computed. Then, correspondent transfer solutions must be computed in a more complete mathematical model including Sun, Earth, Moon and spacecraft.

Indeed, firstly, a scattering region around the Moon is explored performing backward integration of the equations of motion of the full four-body dynamical model, examining different transport processes between regions of the phase space in order to establish debris mitigation routes. For that, sets of initial conditions of lunar osculating orbits are considered, but only initial conditions in a suitable energy range are evolved. We determine which trajectories are orbits that transit from the lunar region and reach the Earth vicinity with slope less than or equal to 5 degrees in relation to the terrestrial equator. This constraint is considered to favor cheaper costs to reach the geostationary orbit that presents zero inclination with respect with the Earth equatorial plane. Then, we will be compute the Δv-budget required to perform the transfer maneuvers from a geostationary orbit to the lunar collision trajectories selected in the previous step using based maneuvers in the Hohmann transfer.[9] And finally, evaluation of the costs of propellant for the accomplishment of the maneuvers found and brief evaluation of the feasibility.

Given these alternative solutions, the number of satellites in cemetery orbits could reduce, decreasing the risk of collisions between a large population of debris in the area, and reducing also objects in an altitude of 35,786 km. These investigations will determine the additional mass of propellant and on-board propulsion systems required for maneuvers for effective and safe mitigation of future generations of communication satellites.

2. Dynamical Model

Two dynamical models are considered in this study: the full N-Body Model (with $N = 4$), accounting for the gravitational attraction of the point-mass Sun, Moon, Earth and spacecraft, and the Spatial Circular Restricted Three-Body Problem (CR3BP). In both cases, the numerical integration is performed by means of RADAU integrator of orders 15.[10,11]

2.1. The N-Body Model

This problem deals with the movement of N bodies subject to mutual gravitational forces. At first, N bodies are considered as point particles with mass m_j different from zero, where $j = 1, ..., N$. By the moment being, we consider four bodies, namely, the Sun ($j = 1$), the Earth ($j = 2$), the Moon ($j = 3$), and the Spacecraft ($j = 4$). Subsequently, the bodies can be considered as spherical masses with their respective mean radius to analyze possible collisions as the distance from one body to the other is smaller than the sum of their mean radii.

From Newton's Law of Universal Gravitation[13] it is possible to describe the equations of motion in the space written in the geocentric reference system $\{0, X, Y, Z\}$. Defining the position vector of the jth body by

$$\boldsymbol{r}_j = X_j \boldsymbol{I} + Y_j \boldsymbol{J} + Z_j \boldsymbol{K}, \tag{1}$$

and the distance between the two bodies j and k given by

$$r_{kj} = \sqrt{\left(X_k - X_j\right)^2 + \left(Y_k - Y_j\right)^2 + \left(Z_k - Z_j\right)^2}. \tag{2}$$

The total gravitational acceleration on a body of mass m_j is given by the sum of the gravitational accelerations of all other bodies $(N-1)$,[7,8] namely,

$$\ddot{\boldsymbol{r}}_j = -\sum_{j=1}^{N} \sum_{k=1;k\neq j}^{N} \frac{\mu_k}{r_{kj}^3} \left(\boldsymbol{r}_k - \boldsymbol{r}_j\right), \tag{3}$$

where, $\mu_k = Gm_k$ with $G = 6.674 \times 10^{-11} N.m^2/Kg^2$ (Universal Gravitational Constant).

Therefore, the gravitational acceleration acting on the Spacecraft by the Sun, Earth and Moon is given by

$$\ddot{X}_4 = -\sum_{k=1}^{N-1} \frac{\mu_k}{r_{k4}^3} \left(X_k - X_4\right), \tag{4}$$

$$\ddot{Y}_4 = -\sum_{k=1}^{N-1} \frac{\mu_k}{r_{k4}^3} \left(Y_k - Y_4\right), \tag{5}$$

$$\ddot{Z}_4 = -\sum_{k=1}^{N-1} \frac{\mu_k}{r_{k4}^3} \left(Z_k - Z_4\right), \tag{6}$$

where

- $\left(X_4, Y_4, Z_4, \dot{X}_4, \dot{Y}_4, \dot{Z}_4\right)$ is the state vector of the Spacecraft (body 4) of mass m_4 in the equatorial reference system centered at the Solar System barycenter, evaluated at a given instant of time.
- $\left(X_k, Y_k, Z_k, \dot{X}_k, \dot{Y}_k, \dot{Z}_k\right)$ is the state vector of the body k of mass m_k in the equatorial reference system centered at the Solar System barycenter, evaluated at a given instant of time.

2.2. The Circular Restricted Three-Body Problem

The CR3BP describes the behavior of a particle with negligible mass moving in the gravitational field of two primaries of masses m_1 and m_2, each revolving around their common center of mass on circular orbits. In this work, m_1 is the Earth and m_2 the Moon. As usual, to remove time dependence from the equations of motion, it is convenient to introduce a synodic reference system $\{O, x, y, z\}$, which rotates around the z-axis with constant angular velocity equal to the mean motion of the primaries. The origin of the reference frame is set at the barycenter of the system and the x-axis the line joining the primaries, oriented in the direction of the smallest primary. In this way, m_1 and m_2 result to be fixed on the x-axis.

The dimensionless variables are chosen to set the sum of the masses of the primaries, the distance between them and the modulus of the angular velocity of the rotating frame equal to 1. In the actual Earth-Moon system, the mutual distance equals 384,400 km (Earth-Moon distance), the unit of the time is 27.32 days, while the dimensionless mass of the Earth+Moon barycenter is $\overline{\mu} = \frac{m_2}{m_1+m_2} = 0.012150582$ with $m_1 > m_2$. The dimensionless masses of the primaries are given by $\mu_1 = 1 - \overline{\mu}$ and $\mu_2 = \overline{\mu}$, the most massive body is located at $(-\mu_2, 0, 0)$, the second one at $(\mu_1, 0, 0)$ (see Fig. 1).

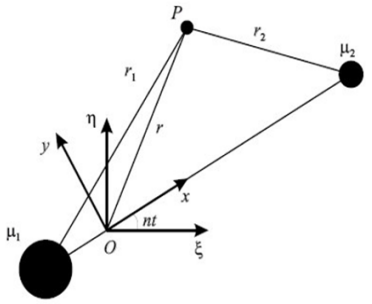

Fig. 1. Planar representation of the Circular Restricted Three-Body Problem in the synodical reference system $\{O, x, y, z\}$ with dimensionless units. The reference system $\{O, \eta, \xi, \zeta\}$ represents the inertial system, fixed in the Earth-Moon barycenter.

Thus, after some algebraic manipulations equations of motion represented in the synodical reference system can be written as

$$\ddot{x} - 2\eta\dot{y} - \eta^2 x = -\frac{\mu_1}{r_1^3}(x + \mu_2) - \frac{\mu_2}{r_2^3}(x - \mu_1), \qquad (7)$$

$$\ddot{y} + 2\eta\dot{x} - \eta^2 y = -\left(\frac{\mu_1}{r_1^3} + \frac{\mu_2}{r_2^3}\right) y, \qquad (8)$$

$$\ddot{z} = -\left(\frac{\mu_1}{r_1^3} + \frac{\mu_2}{r_2^3}\right) z, \qquad (9)$$

where η is the mean motion, $r_1 = \sqrt{(x+\mu_2)^2 + y^2 + z^2}$ and $r_2 = \sqrt{(x-\mu_1)^2 + y^2 + z^2}$ are the distances between the particle P to the two primaries P_1 and P_2, respectively. This system of equations admits a first integral (the Jacobi integral) given by

$$\eta^2\left(x^2 + y^2\right) + 2\left(\frac{\mu_1}{r_1} - \frac{\mu_2}{r_2}\right) - \left(\dot{x}^2 + \dot{y}^2 + \dot{z}^2\right) = C_J, \qquad (10)$$

where C_J is the so called Jacobi constant.[7)] This integral defines a five-dimensional manifolds of the six-dimensional phase space at which trajectories are immersed. This integral of motion also defines the regions of phase space that the particle P can or cannot access. The boundary between the accessible and forbidden regions are the zero velocity surface defined by the zero velocity condition $\left(v = \left(\dot{x}^2 + \dot{y}^2 + \dot{z}^2\right) = 0\right)$ in the Eq. (10). Thus, for each value of C_J, accessible regions are defined in which the motion of the particle is possible. The intersection of these surfaces with the xy plane forms the Zero Velocity Curves.[7,8)] The qualitative study of Zero Velocity Curves is possible using the five values associated with Jacobi Constant at the $L_i, (i = 1, ...5)$ equilibrium points, for which the following relationship holds

$$C_J(L_1) > C_J(L_2) > C_J(L_3) > C_J(L_4) = C_J(L_5). \qquad (11)$$

Figure 2 represents the four distinct configurations defined as a function of the Jacobi constant value. The regions marked in gray are bounded by the Zero Velocity Curves and correspond to non accessible domain. The points P_1 and P_2 represent the center of mass of the primary and the secondary body, respectively, and the $L_i, (i = 1, ...5)$ represent the Langrangian points, where the collinear points L_1, L_2 and L_3 are unstable an the triangular points L_4 and L_5 are stables.

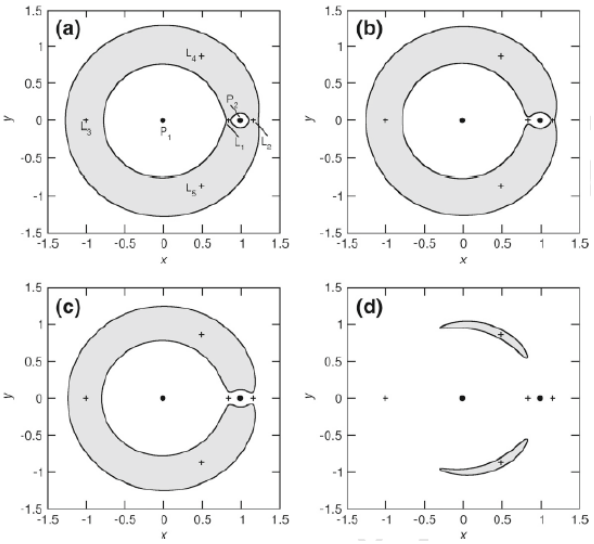

Fig. 2. Distinct configurations of the phase space and zero velocity curves of the Circular Restricted Three-Body Problem for the Earth-Moon system.[12)]

When $C_J \geq C_J(L_1)$, the particle motion is or confined to one of the regions around the primary bodies (called respectively Moon realm and Earth realm), or in the exterior region, as shown in Fig. 2a. If $C_J(L_2) \leq C_J < C_J(L_1)$, the particle can move from one realm to another (Fig. 2b), since a neck around L_1 exists for $C_J < C_J(L_1) = 3,18834$. The particle may escape from the interior regions when a neck around L_2 exists, i.e. for $C_J < C_J(L_2) = 3.17216$, as shown in Fig. 2c. Finally, Fig. 2d exemplifies the cases for $C_J(L_{4,5}) \leq C_J < C_J(L_3)$, when the zero velocity curves shrink, until they cease to exist for $C_J < C_J(L_4) = C_J(L_5)$.

3. Selected Mission and Constraints

The selected mission for the detailed analysis of disposal strategies is Star One C4 (current). The Star One C4 is a Brazilian geostationary communication satellite built by Space Systems/Loral (SS/L).[14)] It is located in the orbital position of 70 degrees west longitude along with Star One C2 and is operated by Embratel Star One, subsidiary of Embratel. The satellite was based on the LS-1300 platform and its life expectancy is 15 years.[15,16)]

Table 1 shows some information about the selected spacecraft used in the study.

Table 1. Spacecraft informations.[15)]

Star One C4 (Hispasat 70W-1)	Values
Position	70° W (70° W)
NORAD	40733
Cospar number	$2015-034B$
Launch data	15/07/2015
Launch Vehicle	Ariane 5 ECA
Launch mass (kg)	5635
Dry mass (kg)	N/A
Orbit	GEO
Expected lifetime	15 years

3.1. Mission scenario

The first stage of our investigation consists on the definition of appropriate sets of initial conditions around the Moon to be backward evolved by natural dynamics in order to seek suitable transfer solutions from the lunar vicinity to the proximity of the Geostationary orbit. So, we generate sets of initial conditions of lunar osculating orbits obtained by varying values of the orbital elements, namely, the semi-major axis (a), eccentricity (e), inclination (i), argument of perigee (ω) and longitude of ascending node (Ω). With this, it is expected to produce solutions that resemble periodic orbits[17)] and quasi-periodic solutions.[18)] More specifically, the orbital elements relative to the Moon are inspected as follows: a is varied from $1,750$ km to $66,750$ km with steps of 130 km; e is varied from 0 to 0.99 with steps of 0.01; i is varied from 0 deg to 15 deg, in steps of 0.4 deg; ω is chosen from 0 to 315 deg, in steps of 45 deg; and Ω is chosen from 0 to 315 deg, in steps of 45 deg.

Each selected initial condition is evolved backward by the full 4-body dynamical model (Eq. (3)) from time equals zero to the final time t_f of $-1,000$ days (so, searched final states of our numerical analysis must correspond to arrival orbits close to the geostationary orbit, that will be the initial states in real time). However, given the huge amount of possible initial conditions to be explored, we adopted a criterion to decide which initial conditions are of interest, reducing the required processing time. For that, we compute the Jacobi constant associated to the Earth-Moon system of each initial condition and select for time evolution only those with C_J in the range between $C_J(L_2)$ and $C_J(L_1)$. With that, considering the good approximate description provided by the CR3BP, we aim to select trajectories that only can transit from the lunar region through the L_1 neck of the Earth-Moon system. It is important to note that the Jacobi constant value in the full 4-body dynamics varies with time and it is used only as a guide for the choice of suitable initial conditions. By the other side, we remark that for initial conditions with inclination close to zero deg, the satellite is very close to the Moon, in such a way that the gravitational forces due to the Earth and the Sun can be considered as small perturbations.

This energy constraint is very convenient as we are searching for transfer solutions from the Earth to the Moon that do not escape the lunar region, with the ultimate goal of a possible collision with the Moon. Indeed, in the context of the CR3BP, this range of energy is the most favorable for low-cost ballistic captured transfers as shown in Refs. (27, 28). As illustrated by Fig. 2b, for $C_J(L_2) < C < C_J(L_1)$, the spacecraft can migrate from the region around the Earth to the region around the Moon through L_1 neck, with the advantage that the zero-velocity surfaces restrict both the accessible region around the Moon and the transit options in the phase space, avoiding, for instance, escape of the trajectory to the exterior region through L_2 and L_3 necks.

Due to the configuration of the initial orbital elements, the initial two-body (2B) energy has a negative value with respect to the Moon (closed orbit). With the time evolution and the perturbation of the third and fourth bodies (the Earth and the Sun), the 2B energy changes its value. When the orbital energy changes to a positive value[19)] (open orbit), this value can be assigned as the capture time of the trajectory. The integration is interrupted if the particle collides with the Moon or the Earth before t_f, or if time exceed $t_f = -1000$ days. If the particle does not escape in the period of $-1,000$ days, its trajectory is called prisoner. However, the cases of interest are those at which the Spacecraft escapes from the Moon vicinity to the Earth region, specially, approaching a Geostationary Orbits (GEO).

Propagating all trajectories candidates to L_1 escape, it will be possible to identify which transit trajectories reach a closest vicinity to the Geostationary Orbit, which is circular and has a radius of approximately $42,164$ km and zero deg inclination in relation to the terrestrial equator. So, seeking suitable transfer solutions, trajectories that reach distances to the center of mass of the Earth lower than $300,000$ km with a inclination equal or lower than 5 deg in relation to the terrestrial equator orbits were selected.

To illustrate the obtained results, Figs. 3 to 5 show the initial conditions selected according to the qualitative dynamical behavior as a function of the semi-major axis, the eccentricity, and the inclination, keeping both $\omega = 90$ deg and $\Omega = 315$ deg constant, for $C_J(L_2) > C > C_J(L_1)$. Figures 3 and 4 present the initial conditions of the trajectories that collide, respectively, with the surface of the Moon and with the surface of the Earth, before t_f is reached. The collisional time in both figures is represented by the color code.

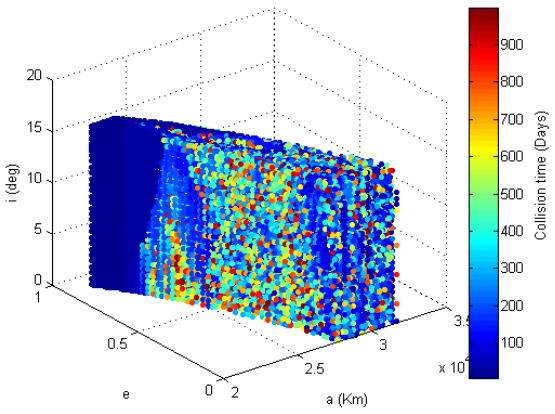

Fig. 3. Trajectories that collide with the Moon surface before t_f as a function of initial values of a, e and i. For these solutions the initial values of $\omega = 90$ deg and $\Omega = 315$ deg are kept constant and Jacobi constants are between $C_J(L_2)$ and $C_J(L_1)$. Color code represents the collisional time.

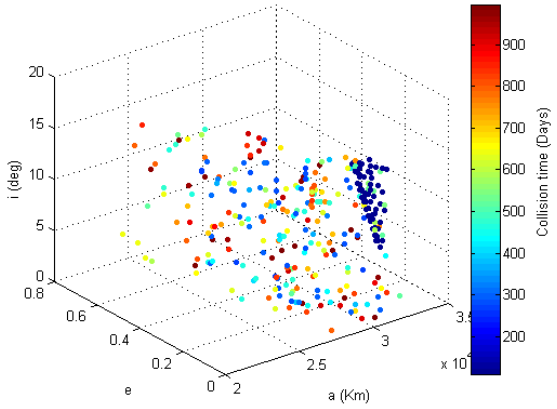

Fig. 4. Trajectories that collide with the Earth surface before t_f as a function of initial values of a, e and i. For these solutions the initial values of $\omega = 90$ deg and $\Omega = 315$ deg are kept constant and Jacobi constants are between $C_J(L_2)$ and $C_J(L_1)$. Color code represents the collisional time.

Figure 5 presents the initial conditions of trajectories that approach geostationary orbits, i.e., reaches a minimum distance to the center of the Earth of $300,000$ km with a inclination in relation to the terrestrial equator i_{24} equal or lower than 5 deg.

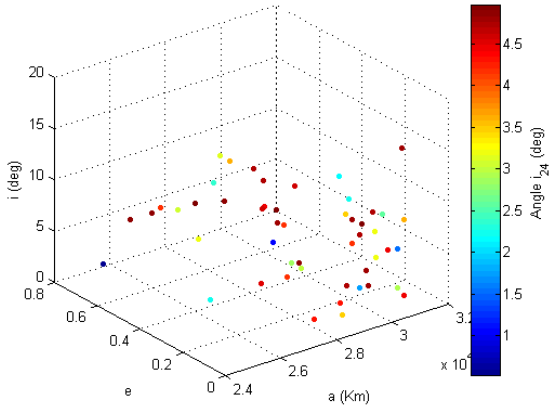

Fig. 5. Trajectories that approach geostationary orbits, i.e., that reach distances to the center of mass of the Earth lower than $300,000$ km with a inclination equal or lower than 5 deg in relation to the terrestrial equator. As in previous figures, solution are presented as a function of a, e and i, for $\omega = 90$ deg and $\Omega = 315$ deg fixed and $C_J(L_1) > C_J > C_J(L_2)$.

The solutions shown in the Fig. 5 are candidates for the mitigation maneuver analysis, outlined in the next Section. In this analysis, we compute the Δv-budget and the amount of propellant needed to perform this disposal maneuver, as well as, a scalar that quantifies the hyperbolic excess velocity with respect to the Moon.

4. Results

In this section, we choose one of the solutions that satisfy the conditions of proximity to the geostationary orbits, shown in Fig. 5, to establish and test a procedure of analysis for design of geostationary satellite disposal. The initial condition of this selected solution is given by $a = 25,150$ km, $e = 0.72$, $i = 1.7$ deg, $\omega = 90$ deg, and $\Omega = 315$ deg. To visualize its dynamical behavior as a function of time, Figs. 6 to 9 present xy projections of the spacecraft trajectory in the synodic system in distinct intervals of time of the full period of 1000 days of retrograde integration. It is possible to observe the escape of the spacecraft through the lagrangian point L_1 in Fig. 8d. The escape occurs approximately on the 598th day of retrograde integration.

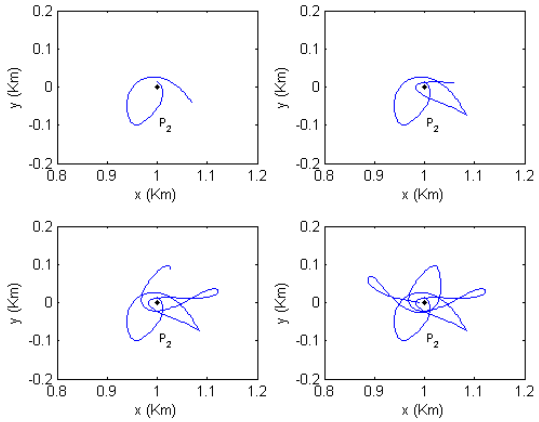

Fig. 6. Projection on xy plane of the synodic system of the selected trajectory from 0 to 167.48 days of retrograde integration.

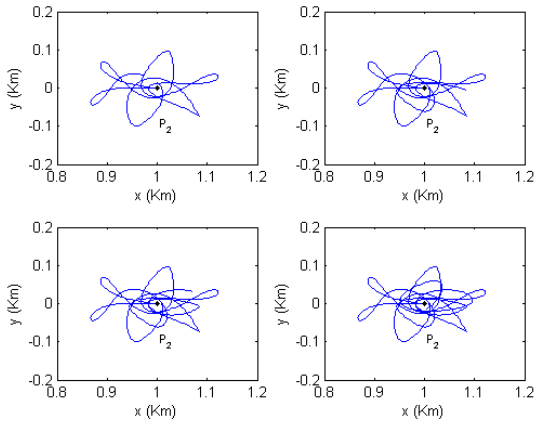

Fig. 7. Projection on xy plane of the synodic system of the selected trajectory from 209.35 to 334.96 days of retrograde integration.

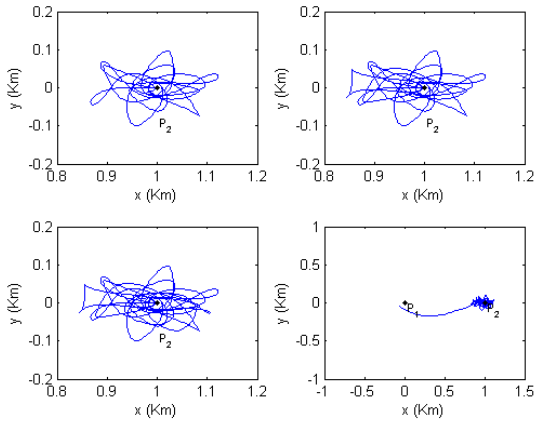

Fig. 8. Projection on xy plane of the synodic system of the selected trajectory from 376.83 to 628.05 days of retrograde integration.

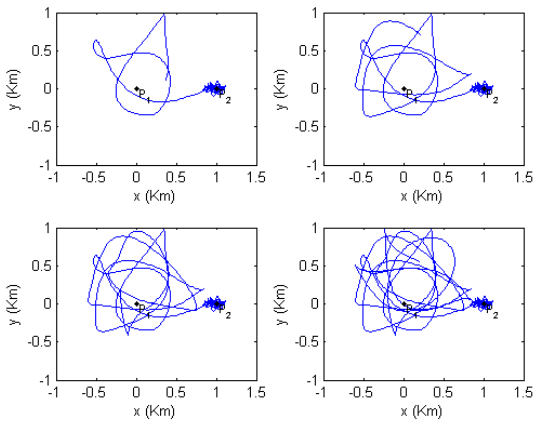

Fig. 9. Projection on xy plane of the synodic system of the selected trajectory from 711.79 to 1000 days of retrograde integration.

The values of the Δv-budget required to perform a transfer from a geostationary orbit to the selected trajectory (shown in Figs. 6 to 9) in different values of instant of time are presented in Fig. 10. Given that, the best instant of time to perform the transfer maneuver for a low-cost transfer can be found. As we are applying a Hohmann transfer, it is required that the satellite is within the sphere of influence of the Moon, because this transfer is based on the problem of two bodies.

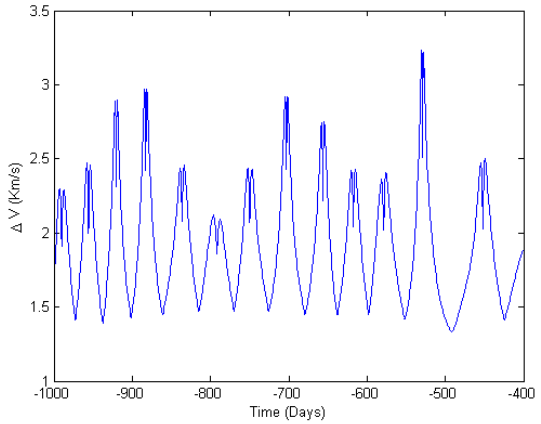

Fig. 10. Δv-budget as a function of the time to leave the Geostationary orbit and reach the selected trajectory of the natural 4B-dynamics.

The propagation of the orbit was performed and for each instant, a Hohmann transfer with three Δv was calculated to transfer the satellite from the location at the 4B-dynamics trajectory to a geostationary orbit. Using Tsiolkovsky's equations[22] the propellant mass required to perform each of the impulses was computed.

In addition, to rank solutions based on characteristics, besides the Δv-budget, the time of flight and the required propellant mass, the half of the hyperbolic excess velocity C_3 may also be used,[5,20] defined as a function of the orbital elements of the state of the spacecraft just before impact as:

$$\frac{1}{2}C_3 = \frac{v^2}{2} - \frac{\mu_3}{r} = -\frac{1}{2}\frac{\mu_3^2}{h^2}\left(1-e^2\right) = -\frac{\mu_3}{2a}, \qquad (12)$$

where v and r are, respectively, the spacecraft velocity and position, h is the angular momentum and e the eccentricity. The C_3 value provides an evaluation of the robustness of the transfer: the lower the value, the more ballistic the capture at the Moon, and thus the more robust the transfer is in case of contingencies. In the case of missing the lunar surface, a trajectory with low C_3 value will be quasi-captured by the Moon allowing for further small maneuvers to impact the spacecraft upon the lunar surface. This value is useful as another parameter to compare one particular transfer with another. Further details on the design strategy of disposal trajectories towards a Moon impact.[21]

Figures 11 to 13 present, respectively, the Hohmann transfer time, the propellant mass required, and the C_3 value together as a function of the flight time. The color code presents also the Δv-budget for the Star One C4.

Given these preliminary analyzes and the examination of the obtained results, we are able to establish more suitable criteria for the selection of solutions for disposal possibilities and then quantify required costs and transfer time for this strategy.

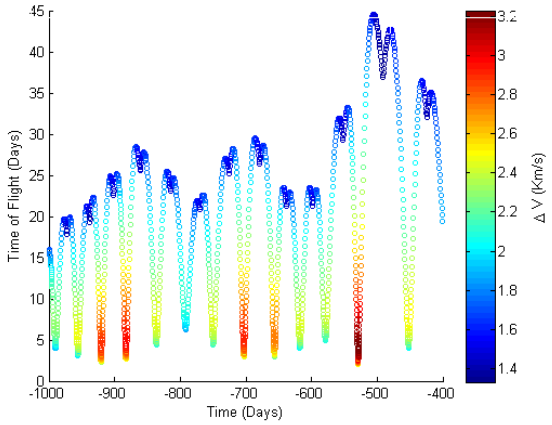

Fig. 11. Hohmann transfer time as a function of the flight time of the $4B$-dynamics trajectory. The color code depicts the required Δv-budget in km/s.

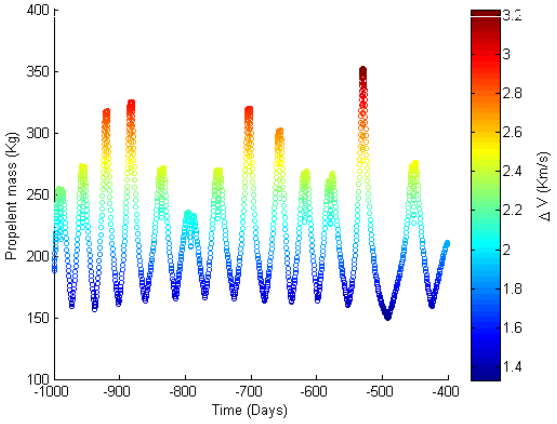

Fig. 12. Propellant mass required as a function of the flight time of the $4B$-dynamics trajectory. The color code depicts the required Δv-budget in km/s.

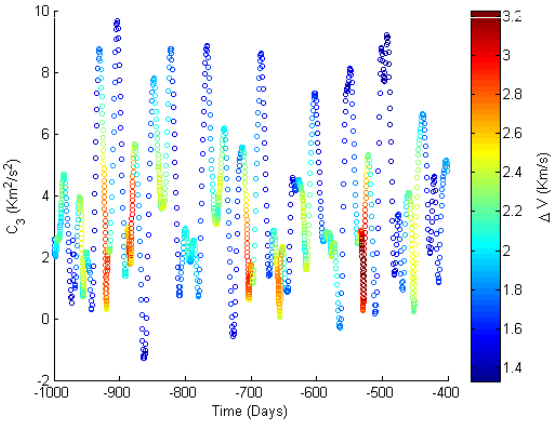

Fig. 13. C_3 value as a function of the flight time of the $4B$-dynamics trajectory. The color code depicts the required Δv-budget in km/s.

5. Conclusion

This paper investigates a strategy to mitigate geostationary missions through lunar impact. The main advantage of considering such disposal option at the end of life is that it removes completely the danger on the space environment that the spacecraft might represent. Compared to transfer to a graveyard orbit (located between 100 and 300 km above the geostationary orbit), this strategy prevents the possibility of an uncontrolled Earth return in a far future. On the other hand, the collision probability within LEO and GEO regions is negligible, because of the low number of excursions within the protected regions (the LEO region in particular).

This work is in agreement with works found in the literature,[3,5] although the Δv-budget required for geostationary missions is larger than for Libration Point Orbit and Highly Elliptical Orbit missions, as expected, since that geostationary orbits are gravitationally captured by the Earth.

In this way, future missions of Geostationary satellites can use this strategy of definitive removal, avoiding the generation of new debris in regions near the geostationary orbit. However, if this maneuver is adopted by a future mission, it will be necessary to perform a study of the probability of collision of this satellite with other debris or even with satellites in operation.

Based on the trend of the current scenario of population growth of space debris and also on increasing interest in missions with geostationary orbits, it is concluded that the maneuvers presented here are alternative to atmospheric reentry maneuvers and, at the same time, more effective than a transfer to an orbit graveyard, because recent studies show the instability of these graveyards orbits that will certainly lead in atmospheric re-entry of such debris to be is not done in a controlled manner can cause disaster if it falls in large urban centers.[3,5]

The main drawback of the disposal strategy presented may be the chaotic nature of the trajectories proposed. In the future, we propose to investigate the role of the uncertainties arising from the orbit determination using Kalman Filter or other estimation method,[23–26] and related to that, the possibility of adding trajectory correction maneuvers to estimated the impact location. Possible evolutions of the work performed also can be included a more detailed analysis of the role of the attitude, and of operations in regard to ground racking and orbit prediction.

The next step is to investigate the second alternative strategy of mitigation, namely, the injection into a heliocentric orbit graveyard,[3] analyzing the Δv-budget and the propellant mass required to carry out this strategy and compare the results with this search.

Acknowledgments

The authors thank the financial support of CAPES-ITA through the grant # 2038/2014.

References

1) NASA Orbital Debris Program Office: Monthly Number of Objects in Earth Orbit by Object Type, *Orbital Debris Quarterly News*, **21**, n.1, (2017), pp. 1 – 14.
2) NASA Orbital Debris Program Office: Monthly Number of Objects in Earth Orbit by Object Type, *Orbital Debris Quarterly News*, **17**, n.1, (2013), pp. 1 – 8.
3) Alessi, L. M.: The reentry to Earth as a valuable option at the end-of-life of Libration Point Orbit missions, *Advances in Space Research*, **55** (2015), pp. 2914–2930.
4) Kessler, D. J. and Cour-Palais, B. G.: Collision frequency of artificial satellites: The creation of a debris belt. *Journal of Geophysical Research*, **83** (1978), pp. 2637–2646.
5) Colombo, C., Alessi, E. M., Van der Weg, W., Soldini, S., Letizia, F., Vetrisano, M., Vasile, M. Rossi, A. and Landgraf, M.: End-of-life disposal concepts for Libration Point Orbit and Highly Elliptical Orbit missions, *Acta Astronautica*, **110** (2015), pp. 298–312.
6) Szebehely V.: *Theory of orbits*, Academic Press, New York, 1967.
7) Murray, C. D. and Dermott, S. F.: *Solar System Dynamics*, Cambridge University Press, London, 1999.
8) Curtis, H. D.: *Orbital Mechanics for Engineering Students*, Elsevier, 2014.
9) Hohmann, W.: *The Possibility of Reaching the Stars*, Verlang R. Oldenbourg, Germany, 1925.
10) Silva, C. N. P. : Numerical Investigation of the Possibilities of Escape of Space Debris trajectories Using Lagrangian Points, Graduate Degree, Federal University of ABC, 2016 (in Portuguese).
11) de Melo, C. F. and Winter, O. C.: Numerical Study About Natural Escape and Capture Routes By Moon via Lagrangian Points L_1 and L_2, *Advances in Space Research*, **40** (2007), pp. 83 – 95.
12) Assis, S. C. and Terra, M. O.: Escape Dynamics and Fractal Basins Boundaries in the Planar Earth-Moon System, *Celestial Mechanics and Dynamics Astronomy*, **120**, n. 2, (2014), pp. 105–130.
13) Newton, I.: *The Mathematical Principles of Natural Philosophy*, Cambridge University Press, London, 1729.
14) Award & Launch History GEO Satellites, http://www.ssloral.com/html/aboutssl/history_1300.html. (accessed Mar. 25, 2017).
15) Star One C4. SatBeams Satellite Details, http://www.satbeams.com/satellites?id=2627. (accessed Mar. 25, 2017).
16) Star One C4. Gunter's Space Page, http://space.skyrocket.de/doc_sdat/staronec4.htm. (accessed Mar. 25, 2017).
17) Broucke, R.: Periodic Orbits in the Restricted Three-Body Problem with Earth-Moon Masses, *JPL Techn. Rep. 32-1168*, 1968.
18) Winter, O. C. and Vieira Neto, E.: Distant stable direct orbits around the Moon, *Astronomy & Astrophysics*, **393** (2002), pp. 661–671.
19) Roy, A. E. and Ovenden, M. W., Monthly Notices of the Royal Astronomical Society, **115** (1955), pp. 296–309.
20) Van der Weg, W. J. and Vasile, M.: Contingency and recovery options for European Student Moon Orbiter, *Acta Astronautica*, **94** n.1, (2014), pp. 168–183.

21) Van der Weg, W. J. and Vasile, M.: Earth-Sun L_1 and L_2 to Moon transfers exploiting natural daynamics, *Proceedings of the 64th International Astronautical Congress*, Beijing, China, IAC-13.C182, 2013.
22) Tsiolkovsky, K., Moore, W. and Academy, R. M.: Tsiolkovsky rocket equation, *Energy*, (1903), pp. 1 – 8.
23) Simon, D.: *Optimal State Estimation: Kalman, H_∞, and Nonlinear Approaches*, Wiley, New York, 2006.
24) Crassidis, J. L. and Junkins, J. L.: *Optimal Estimation of Dynamics Systems*, *CRC Press*, New York, N.Y., 2nd ed., 2012.
25) Silva, W. R., Kuga, H. K. and Zanardi, M. C.: Application of the Extended H_∞ Filter for Attitude Determination and Gyro Calibration, *Advances in the Astronautical Sciences*, (2014), pp. 1501 – 1515.
26) Silva, W. R., Kuga, H. K. and Zanardi, M. C.: Application of the Regularized Particle Filter for Attitude Determination Using Real Measurements of CBERS-2 Satellite, *Advances in the Astronautical Sciences*, (2016), pp. 1343 – 1360.
27) Sousa-Silva. P. and Terra, M. O.: A survey of different classes of Earth-to-Moon trajectories in the patched three-body approach, *Acta Astronautica*, **123**, (2016), pp. 340–349.
28) Sousa Silva, P., Terra, M. O.,McInnes, C., and Ceriotti, M., A heuristic strategy to compute ensembles of trajectories for 3D low-cost Earth-Moon transfers. 67th International Astronautical Congress, Guadalajara, Paper number IAC-16,C1,4,5,x34131, 2016.